Characterization of bimetallic interface in Cu-Al and Ni-Cu rods cold-welded by ECAP

A. P. Zhilyaev[a,b,*], T. Werner[c,d], J. M. Cabrera[c,e]

[a] Laboratory of Mechanics of Gradient Nanomaterials, Nosov Magnitogorsk State Technical University, 455000, Magnitogorsk, Russia

[b] Institute for Metals Superplasticity Problems, Russian Academy of Science, 450001, Ufa, Russia

[c] Dept. Materials Science and Metallurgical Engineering, EEBE, Universitat Politécnica de Catalunya, 08930 Barcelona, Spain

[d] Dept. of Materials Science and Engineering, Universität des Saarlandes, Saarbrücken, Germany

[e] Institute of Metallurgy and Materials, Universidad Michoacana de San Nicolás de Hidalgo, Edificio U, Av. Francisco Múgica s/n, CU, 58230, Morelia, Michoacán, Mexico

* Corresponding author. E-mail: alexz@anrb.ru

Abstract

While cold-welding by equal channel angular pressing has already been confirmed to be a viable alternative to join materials that commonly tend to exhibit unwanted brittleness and other heat induced properties, the exact processes taking place at the interface as well as their effects have not been well studied. In this work, the exact chemical composition along the bimetal-interface has been analyzed by multiple energy-dispersive X-ray spectroscopy line-scans. Furthermore microhardness-

This article has been accepted for publication and undergone full peer review but has not been through the copyediting, typesetting, pagination and proofreading process, which may lead to differences between this version and the Version of Record. Please cite this article as doi: 10.1002/adem.201900653

maps were drawn up based on Vickers-microindentations in the same area. Based on these findings the presence and distribution of intermetallics, as signs of successful welding, were determined, as well as their influence on the mechanical properties of the weld.

Keywords: cold-welding, ECAP, bimetal, microhardness-map, EDX, intermetallics

1. Introduction

For many years now, the welding of dissimilar metals has caused early failure of materials due to thermal fatigue, residual stresses, increased atmospheric corrosion, hot cracking, or massive embrittlement [1, 2]. Through bypassing all these unwanted thermal effects by eliminating high temperatures, cold-welding promises high strength-welds without any loss in mechanical properties [3, 4].

The idea of cold-welding goes back as far as the 1950's, when Parks theorized the possibility of recrystallisation welding without heat [4], and Vaidyanath et al. performed pressure welding by rolling [5]. Since then, many attempts have been made to explain this joining process. However the scientific community remains split. Four of the most recurrent theories are:

- The "Film Theory" [5], which suggests the imperative formation of an oxide layer on the surfaces of metallic materials. This oxide film would have to bebroken through first, the virgin metal subsequently extruding through the cracks until coming into contact with the virgin metal of the second metal subjected to the same condition. Upon contact of these contamination free metals, they would unconditionally weld together. Thus, the thickness of the oxide layer as well as the strain hardening/embrittlement of the surface due to machining of materials are key factors influencing this kind of weld.
- The "Energy-Barrier, based on recrystallisation" [6] promotes the idea of an energy barrier keeping metals from welding together. In this specific case the energy barrier would be the recrystallisation point, as the welding itself would happen in the form of highly deformed interfacial grains recrystallizing, forming a layer of small new grains having a similar microstructure and good physical connection without pores.

- The "Energy-Barrier, based on diffusion" [6] implies that diffusion plays the main role in bonding of two metals. Thus, the key factors here are the diffusion constant as well as the temperature. The higher is the temperature, the more obvious is this effect.
- The "Energy-Barrier, based on grain orientation" [7]. By performing cold welding at 77 K, the temperature of liquid nitrogen, Semenov demonstrated that the key factors are not diffusion or recrystallisation, as these processes were non existent at such low temperatures. Rather he found that the orientation of grains played a major role in cold-welding of two metals. Nevertheless, Semenov recognized that at higher temperatures or higher stresses other effects might come to reinforce this process, otherwise it would be impossible to join polycrystalline materials by cold welding [6].

A few decades ago process equal channel angular pressing (ECAP) [8] was applied for grain refinement in metallic materials leading to an increase in mechanical properties. This process can be employed for welding, which has already been demonstrated for different material combinations such as copper-aluminum [3], aluminum-steel [9], and nickel-copper [10]. It has been suggested elsewhere [10], that cold-welding by ECAP creates intermetallics and oxide particles dispersed along the bimetallic interface by the shear induced during the process, increasing the mechanical properties of the weld. The present work will analyze this idea by means of Vickers microindentation, and chemical analysis via energy dispersive X-ray spectroscopy (EDX) for two types of dissimilar pairs of metals. The first one (Cu-Al) tends to create intermetallic particles during diffusion bonding, and the second one (Ni-Cu) has almost infinite solubility and does not create intermetallic compounds during strain induced diffusion bonding.

2. Materials and Experimental procedures

The chemical composition of the initial materials is listed in Table 1.

Table 1: Chemical composition (mass-%) of the used raw materials

Materials	Chemical elements (mass-%)					
Cu (electrolytic)	Cu	P	Pb	Sn	Ni	Ag
	99.92	0.03	0.02	0.01	0.01	0.01
Ni 201	Ni	Mn	Si	Fe	C	Cu
	99.46	0.25	0.16	0.09	0.02	0.02
Al 6060	Al	Mg	Si	Fe	Cu	Ti
	98.87	0.51	0.36	0.15	0.02	0.01

Two different bimetallic samples (Fig. 1) are subjected to ECAP processing using a 90° split die. Both samples are cylindrical with a 6 mm-diameter core of one metal and an outer shell featuring an external diameter of 8 mm of a second metal.

the Cu-Al combination, where Cu is the outer shell and Al is the inner core. These samples were subjected to 3 ECAP passes at 473 K with a holding time of 18 h to improve diffusion. The ECAP was performed using a "MECAMAQ DE80 Tipo 80" press at a pressing speed of 3 mm/s according to route C [11], meaning the samples were turned by 180° around the longitudinal axis after each pass.

- The Ni-Cu combination, where Ni is the outer shell and Cu is the inner core. The Ni-Cu specimens were processed by 1 ECAP pass at room temperature (RT).

Such combinations (Cu-Al and Ni-Cu) were chosen to perform ECAP bonding on two systems: one (Cu-Al) can easily generate intermetallic compounds, while the second system does not create intermetallic compounds due to infinite solubility. Following the ECAP process, the samples were cut in the longitudinal direction at low speed to avoid excessive heating. The section was grinded and polished for microhardness measurements, optical observation and EBSD analysis. A large-scale microhardness map was produced with indentations in a regular pattern as shown in Fig.2. To avoid overlapping of the deformation zones of each indentation, the chosen load was only 10 g for 15 s, and the distance of one indentation to the next was always larger than three lengths of the diagonal of the

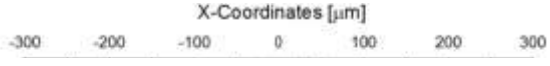

Cu-Al

Ni-Cu

Figure 1. Initial Cu-Al and Ni-Cu specimens prior to ECAP processing.

Figure 2. Schematic representation of the microhardness map of bimetallic-interface region of the sample.

indentation. The indentations were taken as far as 250 μm from the interface, as secondary particles are only expected to be near the interface. Furthermore, it was in[10], that the abnormal increase in hardness is closely centered around the interface.

After determining the areas of interest, the EDX line-scans were performed across these areas to identify the presence of intermetallic phases or oxide particles.

The EBSD analysis was performed only on the Al-Cu specimen subjected to 3 ECAP passes.

3. Results and discussion

3.1 Microhardness mapping

The microhardness maps (Figure 3) obtained distinguish clearly the two sides of the same sample by different values. These results from the different degrees of induced strain depended on the distance to the sharp inner corner of the die. Moreover, it appears that the hardness sharply increases close to the interface. Two main strengthening modes have been observed:a localized increase in specific points in vicinity of the interface, as well as a general increase along the bimetallic junction. While the first can be attributed to small oxide particles broken up and incorporated into the material or grains oriented in an unfavorable direction, the second strengthening mode would be caused by intermetallic/solid solution particles scattered along the interface. The validity of this claim was further investigated in the following section.

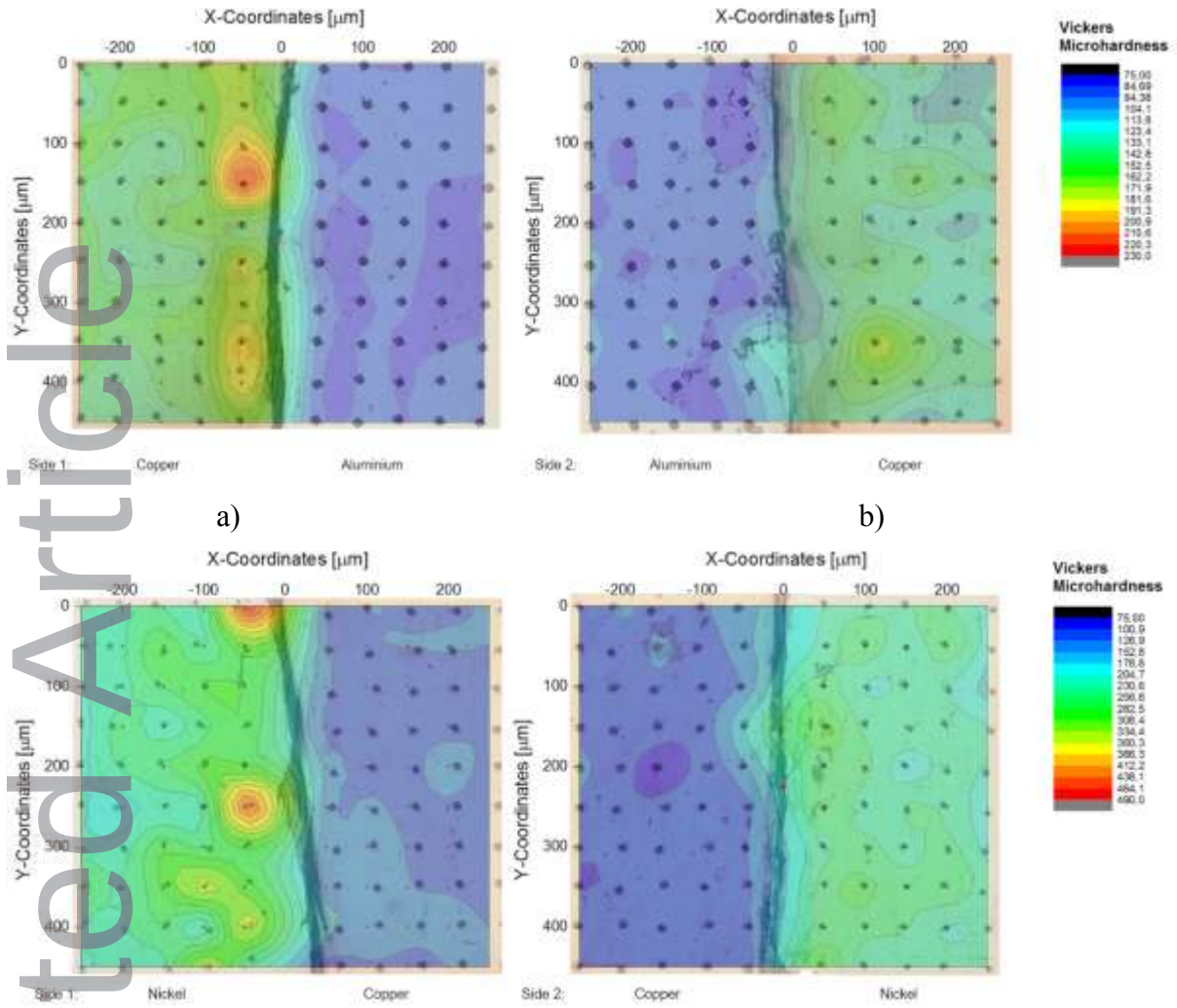

Fig. 3. Microhardness maps close to the (a, b) Cu-Al interface and (c, d) Ni-Cu joint. The left-hand side is a part of specimens which passed near the outer corner and the right-hand side passed near rhe the inner corner of the ECAP die.

Confirming the presence of intermetallics or solid solutes, combined by the increase in hardness at the interface, verifies once more the success of the cold weld. The microhardness measured near the interface can be represented by a simple composite model [12]:

$$Hv_{COMP} = f_{PART} \cdot Hv_{PART} + (1 - f_{PART}) \cdot Hv_{MATR} \qquad (1)$$

where Hv_{COMP} is the hardness of the composite measured close to the interface, Hv_{PART} is the hardness of particles [12], Hv_{MATR} is the hardness of the matrix measured in the bulk material across the whole sample, and f_{PART} represents the volume fraction of particles. It follows from Eq. (1) that f_{PART} can be calculated as

$$f_{PART} = (Hv_{COMP} - Hv_{MATR})/(Hv_{PART} - Hv_{MATR}) \quad (2)$$

These volume fractions were calculated on the basis of the data on common intermetallics found in the copper and aluminum system, as well as the measured data from the microindentations close to the intermetallic interface. The results are summarized in Table 3. The real situation is much complicated, as all types of intermetallic particles may be present in the matrix. Then equation (1) has a more complicated form

$$Hv_{COMP} = \sum f_i \cdot Hv_i + (1 - f_{total}) \cdot Hv_{MATR}, \quad (3)$$

where f_i and Hv_i are the volume fraction and microhardness of Cu_XAl_Y intermetallic particles listed in Table 3.

Table 3. Possible volume fraction of intermetallic particles in Cu-Al depending on the analyzed side of the sample.

Outer corner of ECAP die					Inner (sharp) corner of ECAP die					Comments
Metal	Bulk	Interface	Cu-side	Al-side	Metal	Bulk	Interface	Cu-side	Al-side	
Cu	113	131			Cu	113	175			Experiment
Al_4Cu_9	720		0.030	0.031	Al_4Cu_9	720		0.102	0.023	Calculation
Al_3Cu_4	900		0.023	0.024	Al_3Cu_4	900		0.079	0.018	Calculation
AlCu	900		0.023	0.024	AlCu	900		0.079	0.018	Calculation
Al_2Cu	600		0.037	0.038	Al_2Cu	600		0.127	0.028	Calculation
Al	72	92			Al	72	87			Experiment

One can assume that in the Cu-rich side Al_4Cu_9 particles are predominant in the microstructure and their volume fraction can be as high as 0.03. From the Al- rich side Al_2Cu particles prevail, and a volume fraction of 0.038 of them will be enough to provide the microhardness of H_V=92. The situation is slightly different for the Cu-Al interface of the ECAP billet that underwent the straining around the inner (sharp) corner. First, the microhadness of the Cu side near the bimetallic interface is 30% higher, and the H_V value of the Al side is approximately 5% higher, which is within the experimental error. Similar evaluation gives the volume fraction of Al_4Cu_9 proportionally three times higher for the Cu side, and the volume fraction of Al_2Cu particles is 30% lower.

As for Ni-Cu solid solution, the determination is more complicated, the hardness changes depend on the stoichiometry.

3.2 Energy Dispersive X-Ray Spectroscopy

The EDX line scans were performed across the interfacial region, extending approximately 20 μm into each material. Fig. 4 shows the micrographs with EDX line-scans revealing distribution of the elements for the Cu-Al system. Fig. 5 depicts the micrographs with EDX line-scans revealing

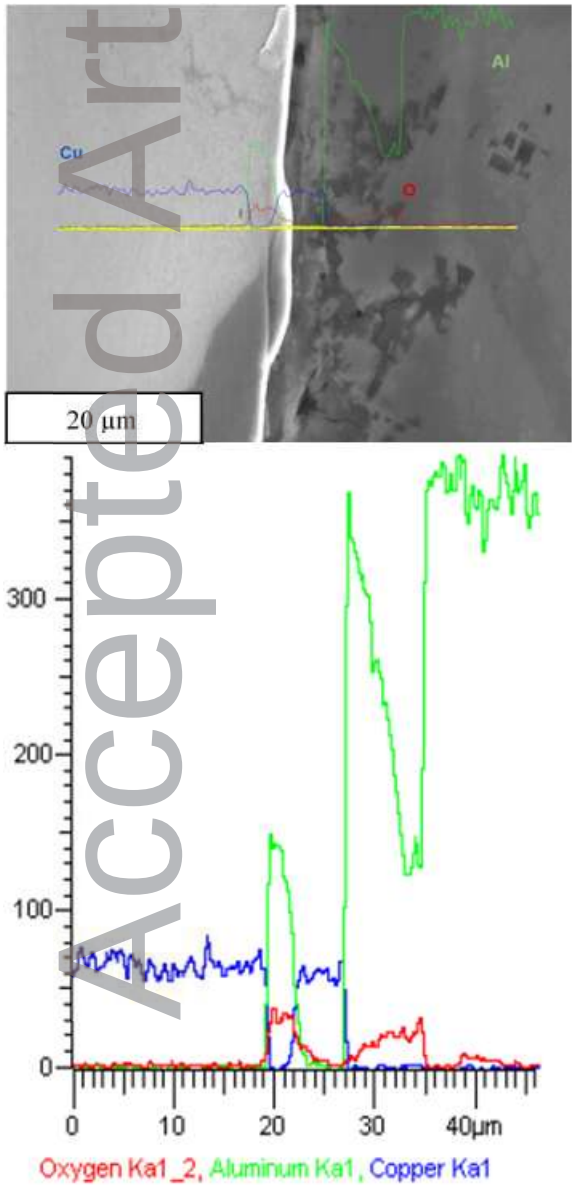

a)

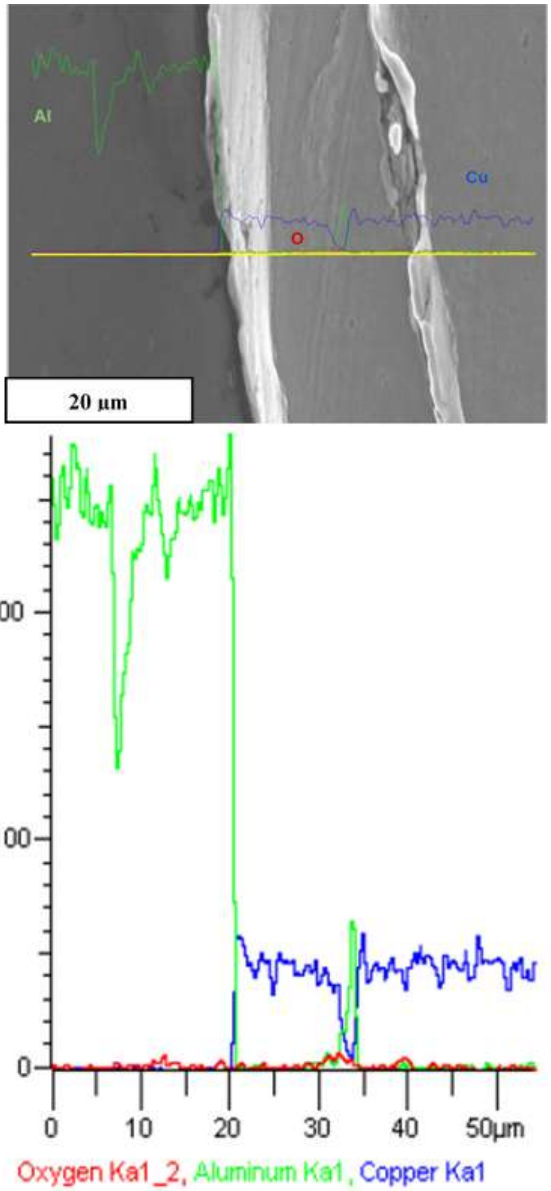

b)

Fig. 4. EDX line-scans showing distribution of elements (Cu, Al and O) across the bimetallic boundary close to the Cu-Al interface: (a) a part of specimens passed outer corner and (b) passed the inner corner of the ECAP die.

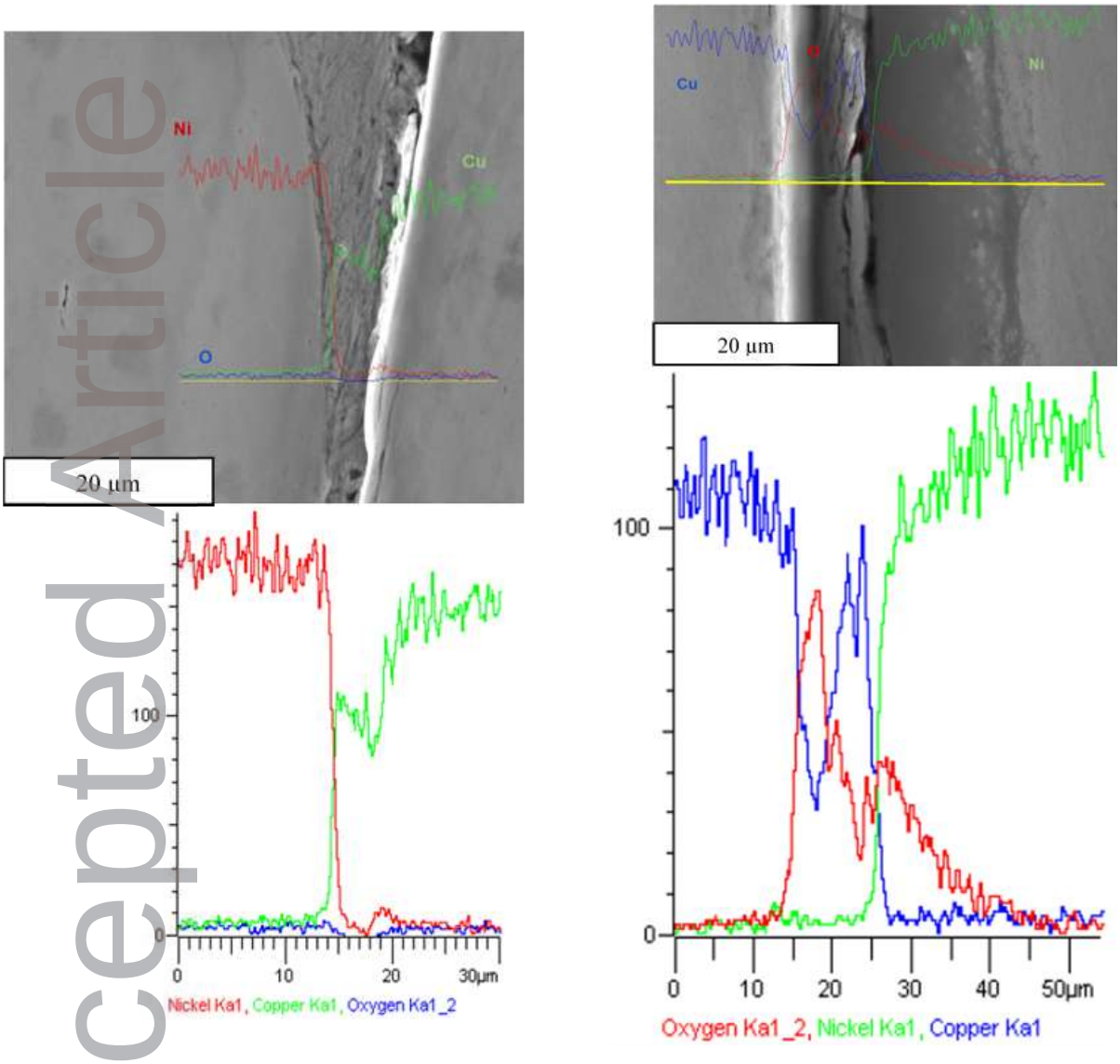

a) b)

Fig. 5. EDX line-scans showing distribution and composition of solid solutes, intermetallics and oxides across the bimetallic boundary close to the (a, b) Cu-Al interface and (c, d) Ni-Cu joint. The left hand side is a part of specimens passed outer corner and the right hand side passed the inner corner of the ECAP die.

distribution of the elements for the Ni-Cu system. The (a) columns in Figs. 4 and 5 correspond to the parts of the samples passed near the outer corner, and columns (b) relate to the parts passed around the inner (sharp) corner.

The intermixing of metals was expected to be a very localized effect along the bimetal boundary, as interdiffusion can span only few nanometers from the interface at the given temperatures and time. (see Table 2).

Table 2. Diffusion parameters and mean diffusion length of the used materials into each other [13, 14]. D_0 is the preexponential coefficient, Q is the activation energy, T is the temperature, D is the diffusion coefficient at the given temperature, $D = D_0 e^{-\frac{Q}{RT}}$. The mean diffusion length is $= \sqrt{4Dt}$.

Solute	**Solvent (host structure)**	**D_0, $\times 10^{-5}$ (m^2/s)**	**Q (kJ/mol)**	**T (K)**	**D (m^2/s)**	**Time (min)**	**Mean Diffusion Length (µm)**
Cu [13]	Ni	2.70	256.0	300	$7.18 \cdot 10^{-50}$	60	$3.22 \cdot 10^{-17}$
Ni [13]	Cu	1.95	236.4	300	$1.34 \cdot 10^{-46}$	60	$1.39 \cdot 10^{-15}$
Cu [14]	Al	1.00	136.0	473	$9.56 \cdot 10^{-21}$	60	$1.17 \cdot 10^{-2}$
Al [14]	Cu	1.00	127.7	473	$7.89 \cdot 10^{-20}$	60	$3.37 \cdot 10^{-2}$

As can be seen in Figures 4 and 5, near the border's regions of around 5-10 µm contain both metals. This confirms the presence of solid solution phases in the Ni-Cu samples, as well as intermetallic particles incorporated into the matrix for the Cu-Al specimen. Furthermore, oxide particles were identified on the interface itself, and also further inside the material. The difference between the calculated diffusion distance and the actual size of the zone, in which both metals were joined can be attributed to the interface not being a straight line, but more of a jagged geometry.

Figures 4 and 5 show that a substantial fraction of the volume is composed of intermetallics or solid solution particles close to the interface, confirming again the success of the weld. These particles do not appear on the SEM image; however, they are represented in the EDX scan as the change in the concentration of the composing elements. This leads to the conclusion that the particles must be of such a small size, e.g. nanosized, that the SEM cannot detect them anymore.

3.2 EBSD microstructure of Cu-Al rod subjected to 3 ECAP passes and hold for 18 hours at 473 K between second and third passes.

Fig. 6 shows the inverse pole figure (IPF) map for the samples that underwent 3 ECAP passes. The samples were held for 18 hours at 473 K, because the plunger broke during the third pass of ECAP, and this was the time to extract the broken plunger. In Fig. 6b, which corresponds to the copper side, large primary grains are subdivided into small grains. The intercept method gives a mean grain size of 4.4 µm and 7.7 µm for copper and aluminum, respectively. The estimation of the geometrically necessarily dislocation density gives approximately identical values for copper side ($1.02 \cdot 10^{14}$ m^{-2}) and aluminum (($1.20 \cdot 10^{14}$ m^{-2}). These are typical magnitudes of dislocation density reported for copper and aluminum processed by ECAP.

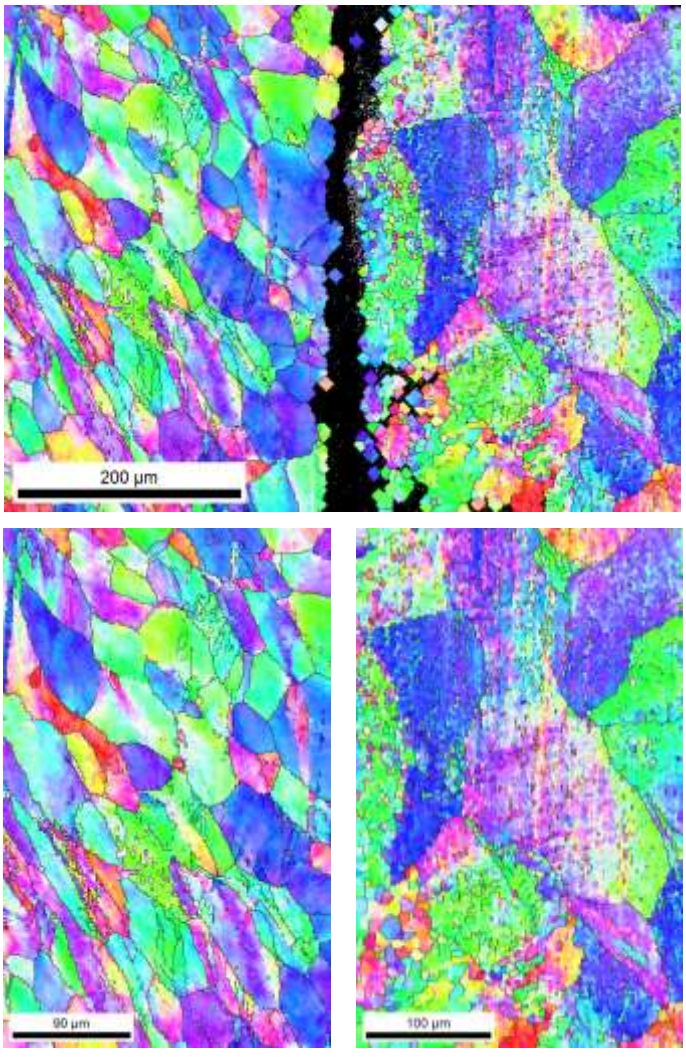

Al-side Cu-side

Fig. 6. IPF maps of the Cu-Al specimen subjected to 3 ECAP passes with intermediate holding at 473 K for 18 hours between 2nd and 3rd passes.

Conclusions

The welding of Cu-Al and Ni-Cu systems was performed using equal channel angular pressing (route C) at room temperature and at T=473K, and the following conclusions can be drawn:

1. Cold welding by ECAP of Cu-Al and Ni-Cu leads respectively to the formation of intermetallic particles and solid solution. However, unlike conventional welding these hard and brittle particles do not lower the mechanical properties of the weld.
2. Due to the nanometric size of the particles and the dispersion along the interface, they act as composite material that strengthens the weld-area.
3. Not all the strengthening comes from the combined hardness of intermetallics/solid solutions and matrix, but also from the restraining effect of the particles on dislocations.

Acknowledgements

This paper is dedicated to the 80th Anniversary of Professor Terence G. Langdon with whom A.P. Zhilyaev and J.M. Cabrera had a long and fruitful collaboration. APZ is grateful to Ministry of Science and Higher Education of Russian Federation for financial support through the grant 074-02-2018-329. JMC is grateful to CONACYT-Mexico for supporting his sabbatical and research stay in UMSNH.

References

[1] D. Bhandari, *Int. J. Inn. Res. Sci. Eng*. **2017**, *3*, 3.

[2] P. Kah, C. Vimalraj, J. Martikainen, R. Suoranta, *Int. Jour. Mech. Mater. Eng.* **2015**, *10*, 10.

[3] N. Llorca, A. M. Escobar, A. Roca, J. M. Cabrera, *Mater. Sci. Forum* **2012**, *706-709*, 1811.

[4] A. R. Eivani, A. Karimi Taheri, *Mater. Let.* **2007**, *61*, 4110.

[5] L. R. Vaidyanath, M. G. Nicholas, D. R. Milner, *Weld. J.***1959**, *6*, 13.

[6] H. A. Mohamed, J. Washburn, *Weld. J.* **1975**, *302*.

[7] A. P. Semenov, *Wear* **1961**, *4*, 1.

[8] A. P. Zhilyaev, R. Z. Valiev, T. G. Langdon, *Bulk Nanostructured Materials: Fundamentals and Applications*, Wiley&Sons, **2014**, p. 450.

[9] Y. Qi, R. Lapovok, Y. Estrin, J. Mater. Sci. 2016, 51, 6860.

[10] T. Werner, *Cold-welding by Equal-Channel Angular Pressing of bimetallic Cu-Al and Cu-Ni rods*, Master Thesis, Universitat Politècnica de Catalunya, **2017**, 102 p.

[11] M. Furukawa, Y. Iwahashi, Z. Horita, M. Nemoto, T. G. Langdon, *Mater. Sci.Eng. A*, **1998**, *257*, 328.

[12] E.S. Puchi-Cabrera, M.H. Staia, A. Iost, *Thin Sol. Films* **2015**, *578*, 53.

[13] B. Dutt et al., *Phys. Stat. Sol.* (a), **1979**, *56*, 149.

[14] *Smithells Metals Reference Book*, 8th Edition (Eds. W.F. Gale and T.C. Totemeier), **2004,** Elsevier, p. 2080.

TOC

The welding of Cu-Al and Ni-Cu systems was performed using equal channel angular pressing (route C) at room and elevated temperature. It leads to the formation of intermetallic particles and solid solution. However, unlike conventional welding these hard and brittle particles do not lower the mechanical properties of the weld.